ACTA ASTRONOMICA
Vol. **63** (2013) pp. 181–201

The Clusters AgeS Experiment (CASE): Variable Stars in the Globular Cluster M4

J. Kaluzny[1], I.B. Thompson[2], M. Rozyczka[1]
and W. Krzeminski[1]

[1] Nicolaus Copernicus Astronomical Center, ul. Bartycka 18, 00-716 Warsaw, Poland
e-mail: (jka,mnr,wk)@camk.edu.pl
[2] Carnegie Observatories, 813 Santa Barbara Street, Pasadena, CA 91101-1292, USA
e-mail: ian@obs.carnegiescience.edu

Received April 25, 2013

ABSTRACT

Based on over 3000 *BV* images of M4 collected in years 1995–2009 we obtain light curves of 22 variables, 10 of which are newly detected objects. We identify four detached eclipsing binaries and eight contact binaries. Accurate periods are found for all but two variables. Nineteen variables are proper-motion members of the cluster, and the remaining three are field stars. Five variables are optical counterparts of X-ray sources. For one of the variables unassociated with X-ray sources we report a flare lasting for about 90 min and reaching an amplitude of $\Delta V = 0.11$ mag.

One of the new contact binaries has a record-low mass ratio $q = 0.06$. Another four such systems show season-to-season luminosity variations probably related to magnetic activity cycles, whose lengths are surprisingly similar to that of the solar cycle despite a huge difference in rotational periods. The location of contact binaries on the color–magnitude diagram of M4 strongly suggests that at least in globular clusters the principal factor enabling EW systems to form from close but detached binaries is stellar evolution. We identify 46 blue and yellow stragglers in M4 and discuss their properties. We also derive a map of the differential extinction in the central part of M4, and determine the reddening of a selected reference region, $E(B-V) = 0.392$ mag.

Key words: *globular clusters: individual: M4 – blue stragglers – binaries: eclipsing – Stars: variables: general*

1. Introduction

M4 = NGC 6121 is located about 1.8 kpc away from the Sun (Kaluzny *et al.* 2013 and references therein) in an uncrowded stellar field at a Galactic latitude of $+16$ deg. These parameters coupled with its low concentration (core and half-light radii of $1\farcm2$ and $4\farcm3$, respectively, Harris 1996, 2010 edition) make it an easy and attractive target for detailed studies, in particular, for a search for variable stars. The online catalog of Clement *et al.* (2001 updated in 2009) contains 80 variables found in the M4 field, of which 50 are either unquestionable or likely RR Lyr stars. The CASE group conducted an extensive search for detached eclipsing binaries in M4, and a detailed analysis of three such system has recently been published by Kaluzny *et al.* (2013). In two earlier contributions (Kaluzny, Thompson and Krzeminski 1997, Mochejska *et al.* 2002) we reported the detection of 15 variables which were located in the blue-straggler region or near the main sequence (MS) on the cluster color–magnitude diagram (CMD). The present paper is a continuation of those studies.

We present the results of the analysis of over 3000 *BV* images collected at Las Campanas Observatory in the years 1995–2009. Section 2 contains a brief report on the observations and explains the methods used to calibrate the photometry. Section 3 is devoted to a measurement of the differential extinction across the M4 field along with the reddening $E(B-V)$ of a selected reference region. The new variables are described in Section 4, and Section 5 is devoted to a discussion of the population of blue/yellow straggler stars in M4. A summary of the paper is contained in Section 6.

2. Observations and Photometric Reductions

The cluster was observed on the 2.5-m du Pont telescope equipped with the TEK5 $2K^2$ CCD camera. All images were taken with the same set of filters at a scale of $0\farcs259$ per pixel. Most of the frames cover an $8\farcm84\times8\farcm84$ field centered $44''$ south and $147''$ east of the cluster center. Observations aimed at covering eclipses of some binary systems involved a subfield of $8\farcm84\times4\farcm42$ centered $31''$ south and $36''$ east of the cluster center. These subrastered images constitute about half of the observations. A detailed log of the observations is accessible at the CASE web page[1].

The data were collected on 51 nights between UT June 1, 1995 and UT June 30, 2009. The images were taken in *V* and *B* filters at a median seeing of $0\farcs99$ and $1\farcs07$, respectively, with average exposures of 47 s for *V* and 102 s for *B*.

In total, we obtained 2447 useful frames in *V* and 672 in *B*. The light curves were extracted with a modified version of the image subtraction utility ISIS V2.1 (Alard and Lupton 1998, Alard 2000). The step involving interpolation of images was performed using the IRAF[2] tasks immatch.geomap and immatch.geotran instead of the interp routine from the ISIS package. DAOPhot, Allstar and Daogrow code (Stetson 1987, 1990) was used to extract the profile photometry of point sources and to derive aperture corrections for reference images. The reference image in *V* was constructed by combining eight individual frames taken one after

[1] *http://case.camk.edu.pl*

[2] IRAF is distributed by the National Optical Astronomy Observatory, which is operated by the Association of Universities for Research in Astronomy, Inc., under a cooperative agreement with the National Science Foundation.

another, each exposed for 19 s. A total of seven B frames were combined, each exposed for 60 s. The seeing for the reference images in V and B was $0\farcs66$ and $0\farcs78$, respectively. For the analysis, each frame was divided into 4×4 or 4×2 segments to reduce the effects of PSF variability.

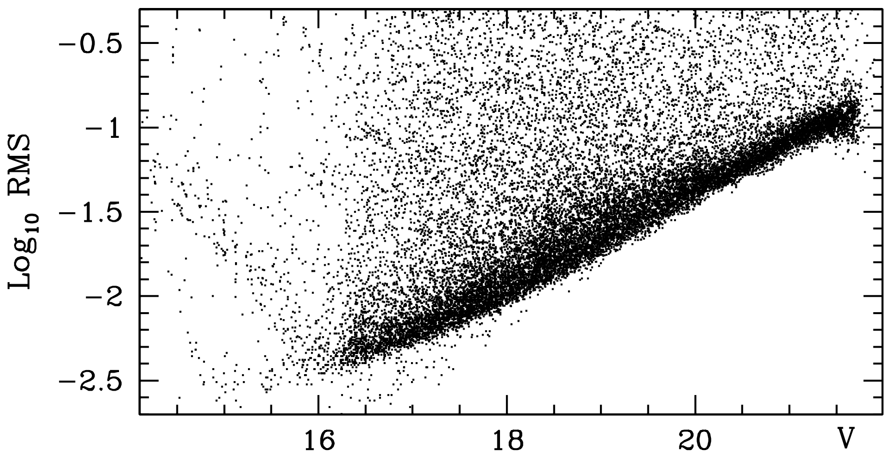

Fig. 1. Photometric measurements of stars in the M4 field. Standard deviation is plotted *vs.* average *V*-magnitude.

The light curves derived with ISIS were converted from differential counts to magnitudes based on profile photometry and aperture corrections determined separately for each segment of the reference images. Instrumental magnitudes were transformed to the standard *BV* system as described in Section 2.1. The V-band light curves were extracted for 15 240 sources. A plot of the *rms* of the individual measurements *vs.* average magnitude for all of the sources is shown in Fig. 1. The photometric accuracy is about 4 mmag at $V=16.0$ mag, decreasing to 49 mmag at $V=20.0$ mag, and to ≈ 100 mmag at $V=22.0$ mag. We note that depending on exposure time and seeing, some images of stars with $14.7<V<16.0$ mag were saturated. The light curves of these objects were carefully filtered to remove points affected by saturation. All stars with $V<14.7$ mag were overexposed on the reference V image, making the study of their light curves impossible.

2.1. Calibration

Accurate calibration of the photometry was essential for the analysis of three detached eclipsing binaries described by Kaluzny *et al.* (2013). To achieve the required accuracy, selected Landolt standards (Landolt 1992) were observed on several nights in different seasons. Two of those observations proved to be of particularly high quality thanks to good seeing and stable transparency. On UT May 2, 2002 we observed 22 standards from five Landolt fields (some fields were observed several times at different airmasses). In total, 82 B and V measurements at air masses $1.07<X<2.00$ were collected. On UT May 5, 2003 we observed 39 standards from seven fields. Again, some fields were observed more than once, totalling 84 B and V measurements at air masses $1.06 < X < 1.94$. Aperture photometry was extracted with DAOPhot, and total magnitudes were derived using Daogrow (Stetson 1987, 1990). Standard magnitudes of stars from Landolt fields were taken from the catalog of Stetson (2000, January 2011 online edition). The following linear transformation from the instrumental (small symbols) to the standard system was derived for UT May 5, 2003:

$$v = V - 0.0112(24) \times (B-V) + 0.1129(40) \times X + \text{const}, \quad (1)$$

$$b = B - 0.0580(27) \times (B-V) + 0.2054(39) \times X + \text{const}, \quad (2)$$

$$b - v = 0.9520(22) \times (B-V) + 0.0979(33) \times X + \text{const}. \quad (3)$$

Fig. 2 shows residual differences between standard and recovered magnitudes and colors, with *rms* values of 0.0091 mag, 0.0086 mag and 0.0071 mag for V, B and $B-V$, respectively. The residuals do not show any systematic dependence on the color index. On the same night several frames of the M4 field were collected at $X = 1.0$ with sub-arcsecond seeing. These data were used to obtain the calibrated BV photometry of the cluster.

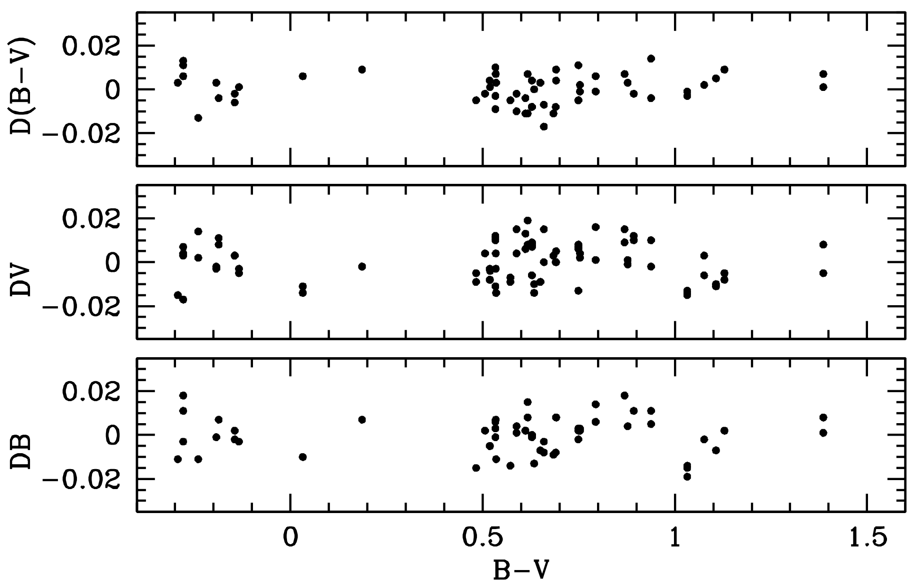

Fig. 2. Residuals resulting from the transformation defined by Eqs. (1)–(3). Difference between original and recovered magnitudes of Landolt standard stars are plotted as a function of color.

For the night of 2 May 2002, we obtained

$$v = V - 0.0133(25) \times (B-V) + 0.1225(30) \times X + \text{const}, \quad (4)$$

$$b = B - 0.0658(27) \times (B-V) + 0.2080(32) \times X + \text{const}, \quad (5)$$

$$b - v = 0.9436(31) \times (B-V) + 0.0904(37) \times X + \text{const}. \quad (6)$$

The *rms* values of the residuals are 0.0077 mag, 0.0077 and 0.0090 mag, for V, B and $B-V$, respectively. As in the previous case, the residuals do not show any correlation with color. On the same night M4 was observed at $X = 1.25$ with sub-arcsecond seeing. Calibrated BV photometry was derived for cluster stars and compared to that from May 5th, 2003. We find that color terms of the two transformations agree with each other to within about one sigma. The average differences of magnitudes and colors calculated for $16 < V < 19$ mag are $\delta V = -0.0132$ mag and $\delta(B-V) = -0.0104$ mag, with 2002 magnitudes brighter and colors redder. The zero points of the finally adopted BV photometry of reference images were chosen as the averages of zero points defined by 2002 and 2003 photometry. The whole observed field contained 83 secondary standard stars from the catalog of Stetson (2000). The average residuals for these stars are $\Delta V = +0.016 \pm 0.0091$ mag and $\Delta(B-V) = 0.0235 \pm 0.0071$ mag, with our magnitudes brighter and our colors bluer.

3. Extinction and Color–Magnitude Diagram

The interstellar extinction exhibits a significant variability across the M4 field (Cudworth and Rees 1990). Maps of differential reddening $\delta E(B-V)$ were derived by Mochejska *et al.* (2002), and more recently by Hendricks *et al.* (2012) and Monelli *et al.* (2013). Hendricks *et al.* (2012) also show that the reddening law for the line of sight toward M4 has the form $A_V/E(B-V) = 3.76$, and that the average reddening in a circle with a $10'$radius around the cluster center is $E(B-V) = 0.37 \pm 0.01$ mag.

The quality of our photometry is high enough to attempt at an independent determination of differential reddening in the observed field. We follow the approach developed by Kaluzny and Krzeminski (1993) in an analogous study of the globular cluster NGC 4372, which later on was reinvented by several other authors. The basic assumption is that the intrinsic width of the principal CMD features (main sequence, subgiant, giant and horizontal branch) is small, and that the cluster is rich enough for these sequences to be densely populated. One may then divide the observed field into segments and derive the differential reddening by shifting their CMDs along the reddening vector until they match each other. Needless to say, such an approach works best when the cluster hosts just one population of stars.

In the case of M4 we split the observed field into an 8×8 mosaic of equal circular subfields with a radius of $65''$, which were partially overlapping. The differential reddening was derived in reference to a 150×150 arcsec^2 square template region centered at $(\alpha, \delta)_{2000} = (245.89109, -26.49646)$ deg. The reddening in this area is nearly uniform, as indicated by the narrowness of main-sequence and subgiant branch on the CMD. We cleaned the template of field stars using the proper motion catalog of Zloczewski *et al.* (2012). From among the remaining cluster members, only those populating main sequence and subgiant branch in a magnitude range 15 mag $< V < 20$ mag were used for the analysis. The merit function used to derive $\delta E(B-V)$ was defined as follows: i) Select a subfield. ii) For each template star select from that subfield stars located closer than 0.04 mag on the $(B-V, V)$ plane. iii) Derive the average distance of those stars from the template star. iv) Sum squared average distances over all stars from the template region. v) Minimize the result as a function of $\delta E(B-V)$.

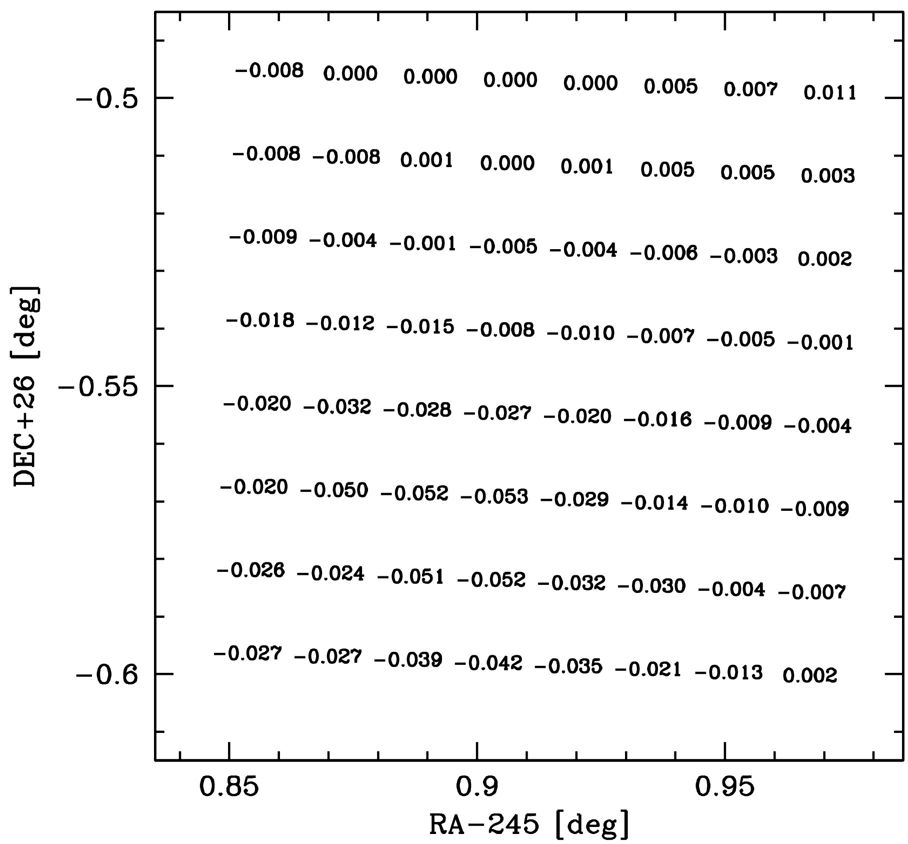

Fig. 3. Differential extinction $\delta E(B-V)$ in the M4 field as a function of J2000 equatorial coordinates.

Fig. 3 is a schematic map of the differential extinction derived for the above quoted reddening law of Hendricks *et al.* (2012). The map in a tabular form is available in the electronic version from the *Acta Astronomica Archive*. The derived values of $\delta E(B-V)$ range from -0.053 mag to $+0.011$ mag, with negative values corresponding to higher reddening. To correct the CMD of M4 for the effects of differential reddening we interpolated $\delta E(B-V)$ for each star. The results of this procedure are illustrated in Fig. 4, whose left panel includes all stars measured on B and V reference images. A sample of stars with $V < 14$ mag and photometry based on a few short-exposure frames taken at a seeing of about $\approx 1''$ is shown to indicate the location of the red giant and horizontal branches. The nearly vertical feature at $(B-V) \approx 1$ mag between $V = 22$ mag and $V = 19$ mag is composed of stars belonging to Milky Way's bulge. The middle panel shows the same CMD corrected for differential reddening and cleaned of objects with relatively poor photometry, which we identified based on the analysis of V/σ_V and V/σ_{B-V} relations. In the right panel only proper motion members of M4 are shown, selected from the middle-panel sample. Note that the proper-motion membership survey of Zloczewski *et al.* (2012) is limited to stars brighter than 21 mag in *V*, and it is very incomplete for bright stars with $V < 13.5$ mag.

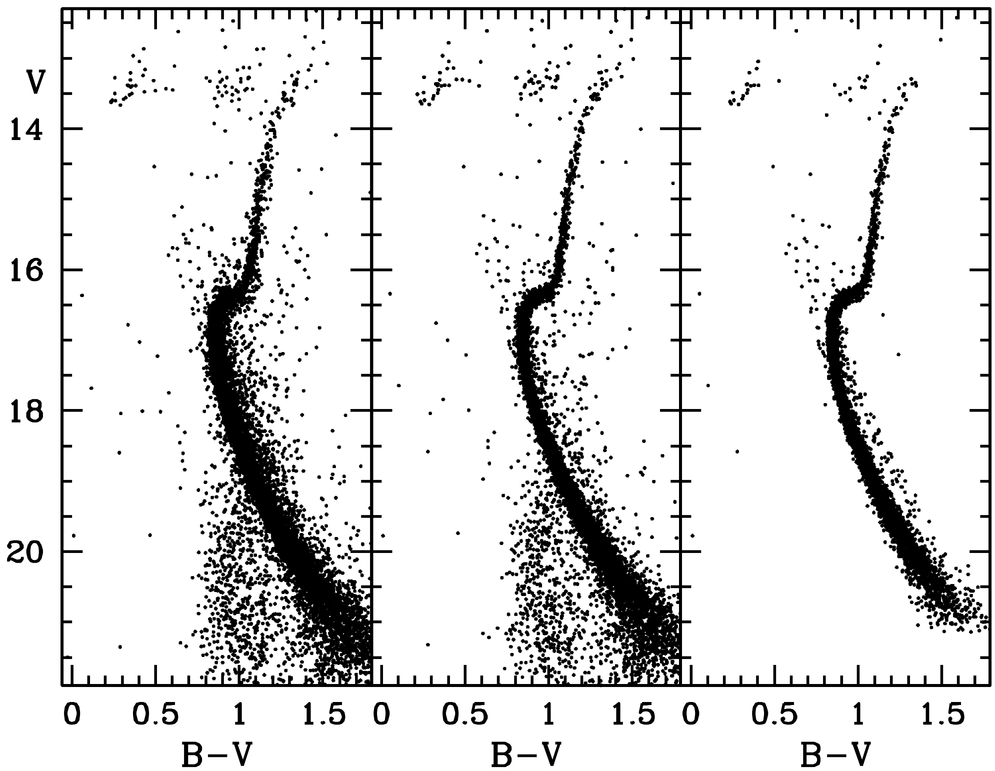

Fig. 4. CMD of M4. In the case of variable objects magnitudes and colors correspond to the phases at which the reference frames were taken. *Left:* all stars, no correction for differential reddening. *Middle:* stars with large errors in photometry are removed; remaining stars are corrected for differential reddening. *Right:* same as middle for proper motion members of the cluster (membership was determined for $V < 21$ mag only).

The reddening for the reference field was derived using the low-extinction globular cluster NGC 6362 as an intermediary. For the latter we obtained *BV* photometry using the same equipment and the same methods as described above. For both NGC 6362 and the reference field of M4 we measured average $B-V$ colors at the turnoff, obtaining 0.5404 ± 0.0004 mag ($rms = 0.0113$ mag, 665 stars) and 0.843 ± 0.001 ($rms = 0.0099$ mag, 85 stars), respectively. The difference in turnoff color, equal to 0.303 ± 0.001, can result from differences in reddening, metallicity and age between the two clusters. According to Dotter *et al.* (2010), M4 and NGC 6362 are coeval at about 12.5 Gyr. This finding is confirmed by our data, since the CMDs of the two clusters match very well when offsets $\Delta(B-V) = 0.303$ mag and $\Delta V = 1.97$ mag are applied.

Three independent surveys (Zinn and West 1984, Carretta *et al.* 2009, Dotter *et al.* 2010) consistently indicate that the difference in [Fe/H] between M4 and NGC 6362 amounts to 0.10, with the latter being more metal rich. Based on Dartmouth Isochrones (Dotter *et al.* 2008) we find that for an age of 12.5 Gyr, and $[\mathrm{Fe/H}] = -1.1$, a metallicity decrease $\Delta[\mathrm{Fe/H}] = 0.1$ causes the turnoff color to decrease by 0.019 mag. According to Harris (1996, 2010 edition) NGC 6362 is reddened by 0.09 mag. This value seems to be a weighted average of $E(B-V) = 0.08$ mag from Reed, Hesser and Shawl (1988) and $E(B-V) = 0.11 \pm 0.03$ mag from Zinn (1985), with both these estimates based on the integrated cluster light. The value we adopt results from the SDF map of the foreground reddening published by Schlegel *et al.* (1998), which at NGC 6362 coordinates gives $E(B-V) = 0.075$ mag. According to Schlafly *et al.* (2010), in regions of low reddening the SDF values of $E(B-V)$ are overestimated by 14%. As a result the reddening of NGC 6362 is reduced to 0.070 mag, and the reddening of our template field in M4 can finally be calculated as $E(B-V) = 0.070 + 0.303 + 0.019 = 0.392$ mag.

4. Variable Stars

We derived *V*-band light curves for 15 240 stars and examined them in a search for variable stars with AOV and AOVTRANS algorithms (Schwarzenberg-Czerny 1996, Schwarzenberg-Czerny and Beaulieu 2006) implemented in the TATRY code. Ten new variables were identified. Our field also contains 13 objects with $V > 15.7$ mag which were previously identified as variables V44–V57. Of these V57 turned out to be constant. Following the numeration from the earlier CASE papers, we named the new variables V58–V56 and V68. Variable V67, discussed by Kaluzny *et al.* (2013), is not included here because it is located outside the observed field. Equatorial coordinates of all 22 confirmed variables are listed in Table 1.

The astrometric solution for the reference image in *V* was found based on positions of 273 UCAC3 stars (Zacharias *et al.* 2010). The average residuals in RA and DEC between cataloged and recovered coordinates amount to $0\farcs00 \pm 0\farcs13$ and $0\farcs00 \pm 0\farcs13$, respectively. Finding charts for V44–V56 can be found in Kaluzny *et al.* (1997). The finding chart for V63 was published by Mochejska *et al.* (2002), who, however, did not detect its variability, and classified it as a blue object, named B3. Based on the photometric data described here and an extensive spectroscopic survey, variables V65 and V66 were examined in detail by Kaluzny *et al.* (2013), who also provide the relevant finding charts. The remaining seven charts for the new variables are presented in Fig. 5.

Table 1

Equatorial coordinates of M4 variables identified within the present survey

ID	RA(J2000) [deg]	Dec(J2000) [deg]	ID	RA(J2000) [deg]	Dec(J2000) [deg]
44	245.83760	−26.55700	56	245.89282	−26.49887
46	245.94653	−26.53236	58	245.89228	−26.52629
47	245.85642	−26.48659	59	245.91317	−26.49859
48	245.90328	−26.52891	60	245.94794	−26.53663
49	245.89301	−26.53384	61	245.92637	−26.55500
50	245.88047	−26.53015	62	245.88582	−26.60363
51	245.88830	−26.51918	63	245.86390	−26.54075
52	245.88111	−26.51607	64	245.83658	−26.51727
53	245.91034	−26.53635	65	245.86826	−26.50608
54	245.96223	−26.57836	66	245.88431	−26.52813
55	245.94067	−26.52127	68	245.91071	−26.50860

Objects V45, V57, and V67 are not listed here as the first one turned out to be constant, and the second one is located outside the field analyzed in this paper.

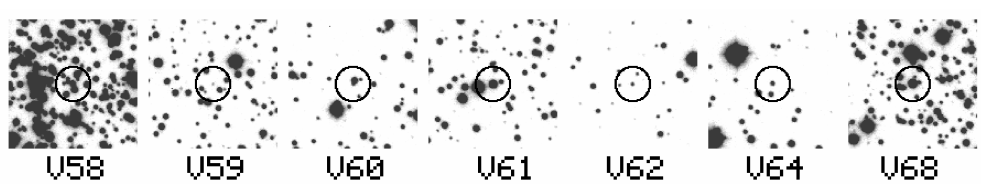

Fig. 5. Finding charts for variables V58–61, V62, V64, and V68. Each chart is 30″ on a side, with North up and East to the left. See text for references to charts published elsewhere.

To check on the effect of blending on the photometry of our variables, we examined HST/ACS images of M4 and the catalog of Anderson *et al.* (2008). V48 has three close visual companions located at distances of 0.″21 to 0.″84. We measured profile photometry for this quadruplet in the fixed-position mode using positional information extracted from the data of Anderson *et al.* (2008). The detached binary V65 has two close visual companions at distances of 0.″37 and 0.″57. Their presence was deduced from the ground-based data, but accurate coordinates could only be determined based on HST/ACS photometry. The case of V58 was discussed in detail by Kaluzny *et al.* (2012). This $V \approx 20.5$ mag optical counterpart to the X-ray source M4-CX1 (Bassa *et al.* 2004) has a bright companion at a distance of 0.″15 which we originally regarded to be the source of variability. A closer analysis unambiguously showed that the fainter component of the blend is responsible for the observed variations. As far as can be established based on HST/ACS data, the images of the remaining variables are free from significant blending problems.

The basic properties of the variables are listed in Table 2. The periods in column 2 were derived with the help of the above mentioned code TATRY. In the

Table 2

Basic data of M4 variables identified within the present survey

ID	P [d]	V_{max} [mag]	$B-V$ [mag]	ΔV [mag]	$\Delta E(B-V)$ [mag]	PM[a]	Type[b]
44	0.263584542(2)	17.746	0.987	0.19	-0.020	Y	EW
46	0.0871525535(3)	18.553	0.287	0.05	-0.005	Y	sdB
47	0.269874785(2)	16.826	0.815	0.27	-0.005	Y	EW
48	0.28269398(2)	16.805	0.812	0.31	-0.005	U	EW CX15
49	0.297443902(1)	17.087	1.290	0.99	-0.007	N	EW CX13
50	0.26599834(1)	17.251	0.830	0.48	-0.006	Y	EW
51	0.303682374(3)	17.103	0.870	0.45	-0.001	Y	EW
52	0.7785087(15)	16.863	0.950	0.13	-0.003	Y	-
53	0.308448705(1)	15.757	0.594	0.23	-0.007	Y	EW
54	0.25244661(1)	17.802	0.951	0.24	-0.008	Y	EB
55	0.310703451(1)	16.722	0.809	0.41	0.001	Y	EW
56	–	14.646	1.154	0.14	0.000	Y	CX5 CX9
58	0.2628216(1)	20.38	–	0.35	-0.001	U	CX1
59	0.71155962(4)	20.296	1.565	0.41	0.000	Y	EA
60	0.370342607(7)	19.297	1.206	0.51	-0.005	Y	EA
61	0.0413287(1)	15.683	0.590	0.01	-0.014	Y	SX
62	0.04062724(10)	19.074	0.608	0.07	-0.040	N	SX
63	–	17.670	0.101	0.03	-0.012	Y	sdB?
64	0.040953844(9)	18.439	0.609	0.05	-0.008	N	SX
65	2.29304564(26)	17.028	0.903	0.40	-0.006	U	EA CX30
66	8.11130346(85)	16.843	0.878	0.70	-0.003	Y	EA
68	0.0380887(1)	15.238	0.615	0.01	0.000	Y	SX

Notes: [a] Membership status: Y – member, N – field star, U – unknown; [b] EW – contact binary, EB – close eclipsing binary, EA – detached eclipsing binary, SX – SX Phe type pulsator, CX – X-ray source from Bassa *et al.* (2004), sdB – hot subdwarf.
Variables V58–V66 and V68 are newly detected. Objects V57 and V67 are not listed here as the first one turned out to be constant, and the second one is located outside the field analyzed in this paper.

case of the eclipsing binaries the $(B-V)$ values in column 3 correspond to the phase of maximum brightness. For the remaining stars we provide median $(B-V)$ from all available measurements. Column 6 contains differential corrections to the reference reddening of 0.392 mag. They are interpolated from the map shown in Fig. 3. The membership status in column 7 is taken from the proper motion study of Zloczewski *et al.* (2012). It is worth noting that in their Fig. 1 members of M4 are very clearly separated from field stars. The classification of the variables as well as associated X-ray sources discovered by Bassa *et al.* (2004) are given in column 8. The optical variables were identified with X-ray sources based on positional coin-

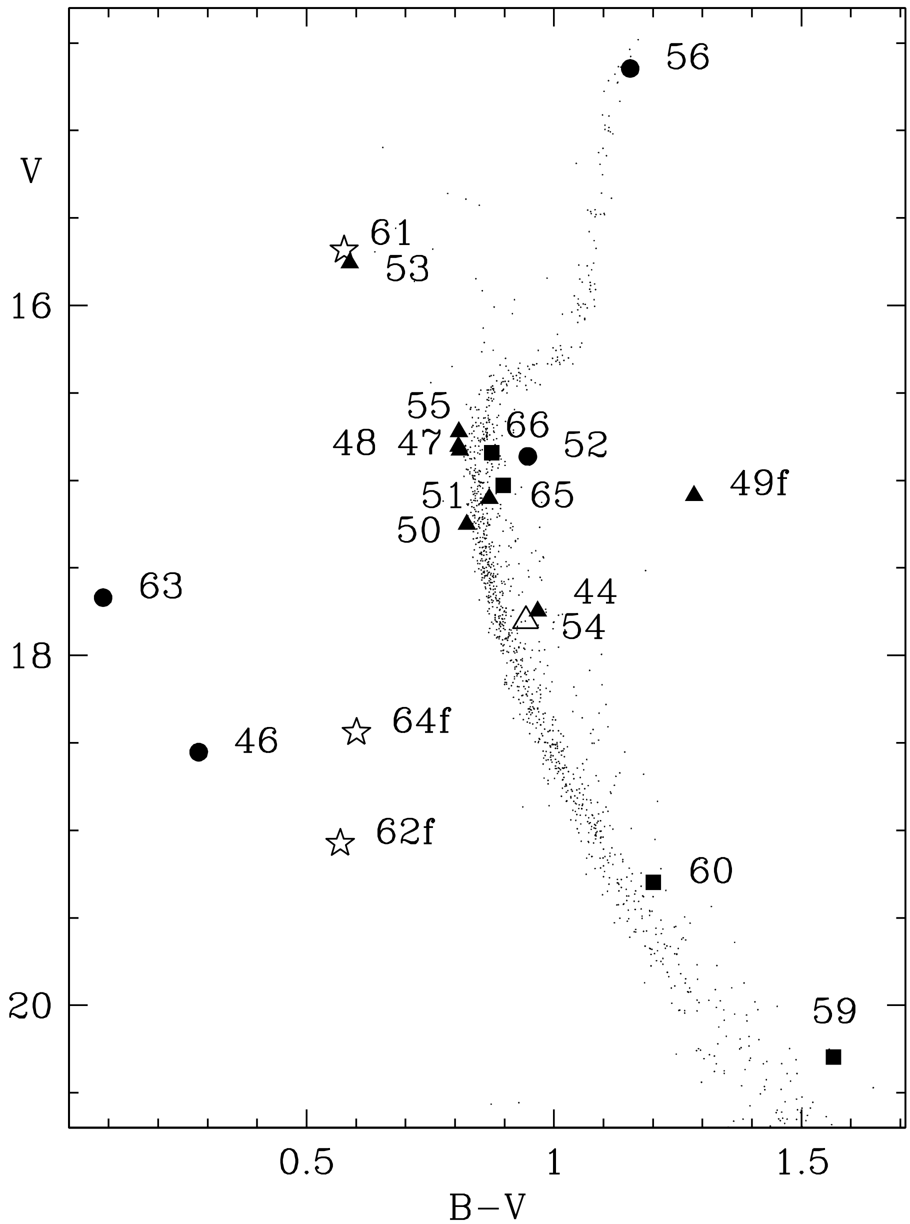

Fig. 6. CMD of M4 with positions of variables detected within the CASE program. Magnitudes and colors of the variables are taken from Table 2, *i.e.,* they either correspond to the phase of the maximum brightness or are median values from all measurements. Squares: detached binaries; triangles: contact binaries; stars: SX Phe variables (field objects are marked with "f"). Background dots: non-variable stars selected from a small section of the observed field to avoid crowding.

cidences. In all cases but one the identification was unambiguous. The exception was V56, located between X-ray sources CX5 and CX9 which are separated by $1\farcs3$. Positions of variables on the CMD of M4 are shown in Fig. 6.

4.1. Eclipsing Binaries

The sample of variables includes thirteen eclipsing binaries. All but one of these are likely proper motion members of the cluster. Their phased *V*-light curves are presented in Fig. 7. In four cases the light curve indicates a detached configuration. Variables V65 and V66 are located at the cluster turnoff. A detailed analysis of these two systems, including a determination of absolute parameters and ages, was presented in Kaluzny *et al.* (2013). The faint binary V59 is located ≈ 0.7 mag

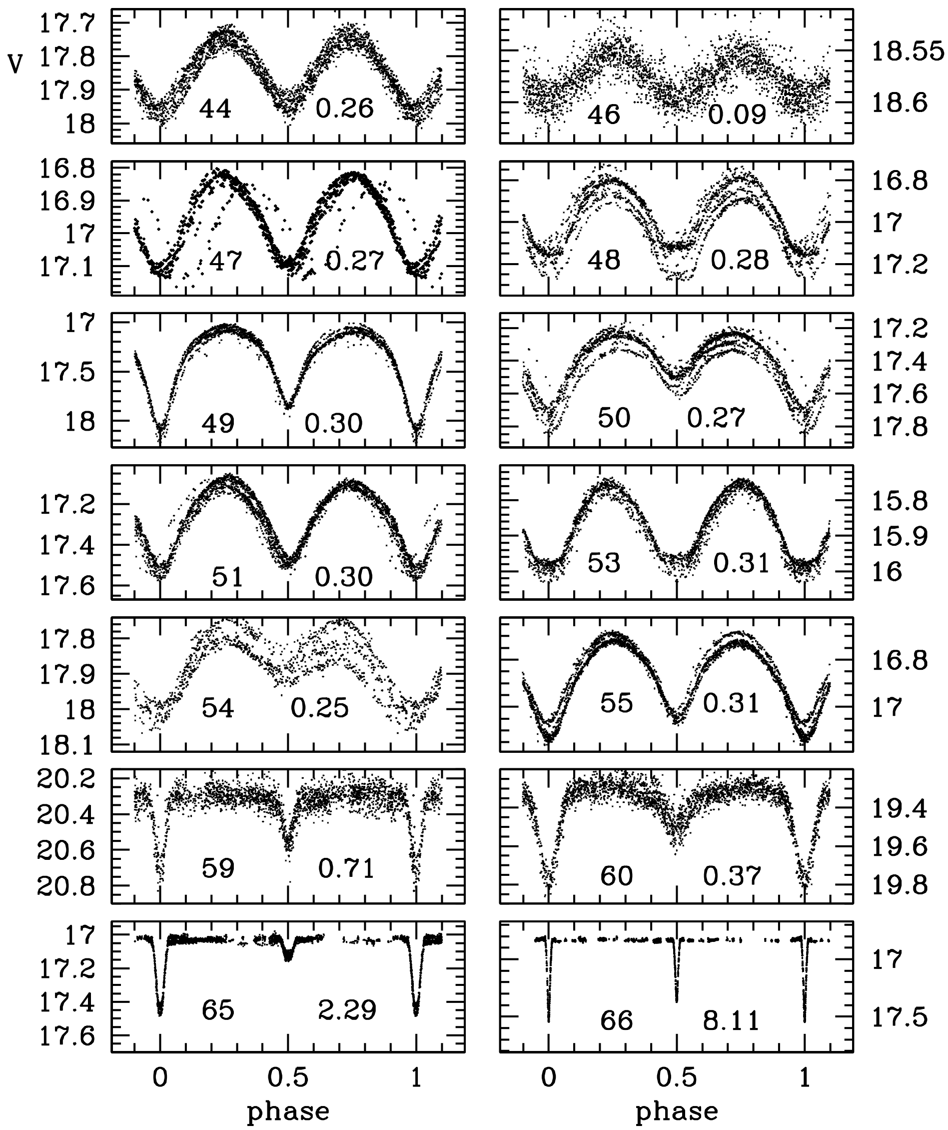

Fig. 7. Phased *V*-light curves of eclipsing binaries and the ellipsoidal variable V46. In each panel the left label gives the name of the variable (with V omitted to save space), and the right one the orbital period in days.

above MS which indicates that its mass ratio is close to unity. The light curve of V60 shows noticeable curvature between the eclipses. Despite the rather short orbital period of 0.37 d this system is undoubtedly detached. This conclusion is based on a preliminary analysis of the light curve performed with the PHOEBE utility (Prŝa and Zwitter 2005).

The remaining nine eclipsing variables are classified as contact binaries (EW). All but V49 have proper motions consistent with cluster membership. Two systems, V50 and V54, show a particularly large difference between the depths of primary and secondary eclipses. Such light curves are called EB-type, and sometimes they are observed in semidetached binaries. Since the eclipses of V50 and V54 are partial, and the mass ratios are unknown, we cannot exclude that these two systems are semidetached rather than contact. However, their short orbital periods favor the second possibility (in particular, the light curves of V50 and V54 can be reproduced assuming a contact configuration and modest mass ratios of ≈ 0.3).

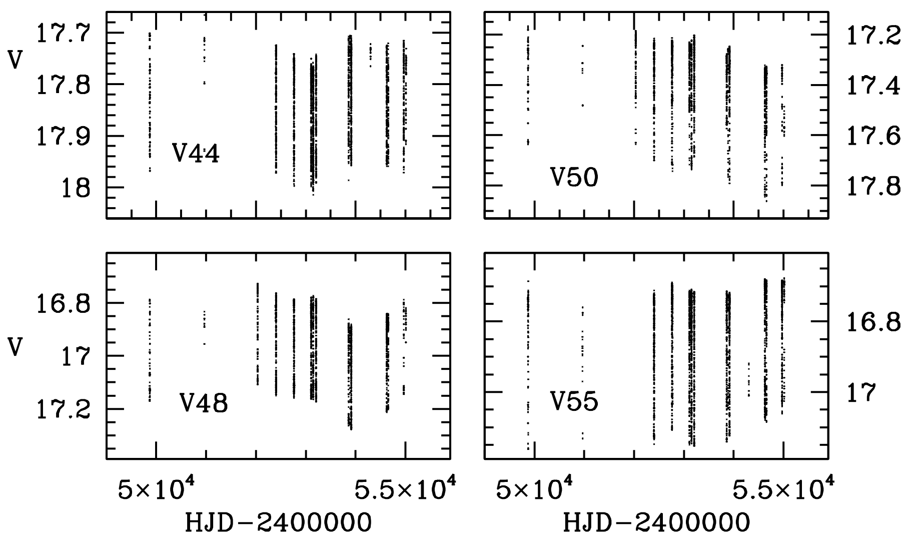

Fig. 8. Light curves of stars V44, V48, V50, and V55.

All but possibly one of the EW systems show season-to-season variations of the average luminosity. Particularly large and systematic variations occur at all orbital phases in V44, V48, V50, and V55, where the whole light curve varies by more than 0.1 mag (see Fig. 8). Analogous behavior is observed in V54 (see Fig. 7), but the changes are less systematic. Similar effects were reported and discussed by Rucinski and Paczynski (2002) in an EW system observed during three consecutive seasons by the OGLE team, and it would be certainly worthwhile to analyze in this respect the sample of 569 contact binaries observed by OGLE during 14 seasons (Kubiak, Udalski and Szymański 2006). Such luminosity variations can be explained by magnetic cycles analogous to the Solar cycle. The length of the cycle is about 5 years in V44, 8–9 years in V48 and V55, and more than 9 years in V50. It is interesting that while our EW systems rotate two orders of magnitude faster than the Sun, their magnetic activity periods do not vastly differ from the solar period. Finally, we note that several EW systems in M4 show evidence for orbital period variability, with particularly rapid changes occurring in V47 and V50. A detailed analysis of this effect is, however, beyond the scope of the present paper.

Our survey of the contact binaries in M4 leads to two interesting conclusions. First, that EW systems are absent among unevolved cluster stars. On the CMD of the cluster they begin to appear about 1 mag below the turnoff, at $V \approx 17.8$ mag and $B-V \approx 0.95$ mag. These values correspond to $M_V = 5.0$ mag and $(B-V)_0 = 0.55$ mag, which at an age of ≈ 12 Gyr implies primary masses of about 0.7 $M_\odot$. Moreover, five out of the seven contact binaries belonging to the MS are located within ≈ 0.3 mag from the turnoff, and not a single such system was detected among 12 246 stars with $17.8 < V < 21$ mag whose light curves we analyzed. Fig. 1 makes it obvious that we would detect all EW variables down to $V \approx 22$ mag with light curve amplitudes larger than 50 mmag. And indeed, there are numerous binaries in M4: the right panel of Fig. 4 shows a well populated sequence parallel to the MS which is most simply interpreted as a binary sequence. These two findings indicate that at least in globular clusters the principal factor enabling EW systems to form from close but detached binaries is stellar evolution. A similar conclusion results from the studies of variables in M55 (Kaluzny *et al.* 2010) and NGC 6752 (Kaluzny and Thompson 2009). Apparently, even modest stellar evolution is more important in this respect than the frequently invoked mechanism of magnetic breaking; see *e.g.*, Stępień and Gazeas (2012) and references therein.

The second conclusion concerns the frequency of contact binaries among evolved MS stars in M4. W UMa variables of spectral types F–G are common in the nearby thin disk population. Rucinski (2002) estimated that in the solar neighborhood their frequency relative to the MS is as high as 0.2%. A similar frequency was found for the thick disk population by Nef and Rucinski (2008). In M4 we detected seven contact binaries among 5652 upper MS stars with $16.5 < V < 18$ mag. The corresponding relative frequency of occurrence, $0.12 \pm 0.05\%$, is consistent with that found for field stars.

The eclipses in V48 and V53 systems are total (Fig. 7). Mochnacki and Doughty (1972) demonstrated that the totality of eclipses in a contact binary allows for a reliable determination of two otherwise degenerate parameters: mass ratio q and inclination i. We analyzed the V-light curves of V48 and V53 with PHOEBE, obtaining $q = 0.148$ and $q = 0.060$ for V48 and V53, respectively. The latter result is very interesting as it sets a new record-low mass ratio, beating SX Crv with $q = 0.066 \pm 0.003$ measured spectroscopically by Rucinski *et al.* (2001). Mass ratios that low pose a challenge for the current theory which predicts $q = 0.09 - 0.08$ as the lower limit for tidally stable contact binaries (Rasio 1995, Arbutina 2012). A detailed analysis of V48 and V53 is deferred to a separate paper.

4.2. Other Variables

Variable objects V53, V61, and V68 belong to the group of blue stragglers discussed in Section 4.3. The first one was described above. The remaining two are pulsating stars of SX Phe type. They belong to the bluest of all M4 stragglers and are apparently located at the red boundary of the instability strip for M4 metallicity of $[\mathrm{Fe/H}] = -1.16$ (Harris 1996, 2010 edition). We note that the analysis of blue straggler populations in several globular clusters would allow an empirical determination of instability strip limits for SX Phe stars as a function of metallicity. We detected two additional SX Phe stars (V62 and V64), which, however, are field objects. Their observed magnitudes indicate that they are located in the Galactic halo or the outskirts of the bulge, far behind the cluster.

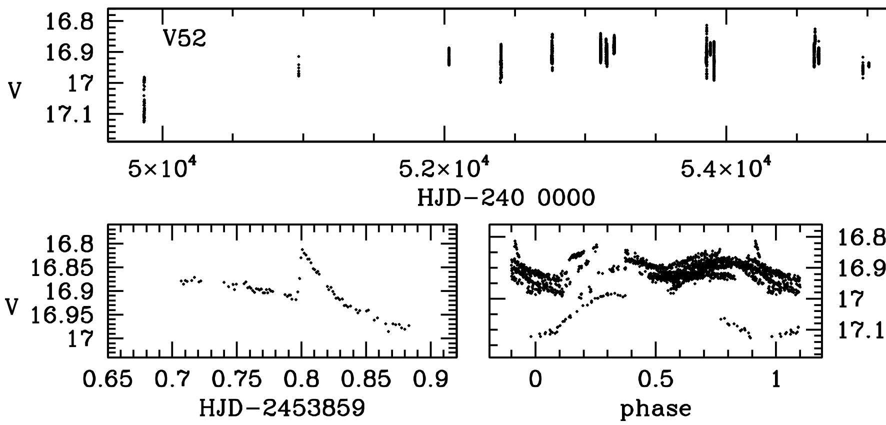

Fig. 9. Time-domain and phased light curves of the variable V52 in *V*-band.

The variable V52 is a proper motion member of M4. Located 0.1 mag to the red of the main sequence, it can be called a red straggler. In Fig. 9 we show its time-domain and phased light curves. The average luminosity of V52 varies from season to season. A superimposed periodic variability with $P \approx 0.78$ d is also observed. Both the shape of the light curve and its coherence over the interval of 14 years indicate that we are dealing with a binary star. The observed periodic modulation may be due to the ellipsoidal effect. On UT May 3, 2006 a flare of V52 was observed, lasting for about 90 min and reaching an amplitude $\Delta V = 0.11$ mag (Fig. 9). Optical flares are often observed in close binaries with chromospherically active components. The chromospheric activity should be accompanied by an X-ray emission. However, none of the X-ray sources detected in M4 by Bassa *et al.* (2004) coincides with V52. Since the variable is located ≈ 1.0 mag above the main sequence, it cannot be composed of two main sequence stars. As such, it deserves a spectroscopic follow-up aimed at the determination of its nature.

The variable red giant V56 is a proper motion member of M4. As can be seen in Fig. 10, in addition to seasonal variations of the average luminosity it exhibits a low amplitude variability on a time scale of ≈ 10 days. The star may be as-

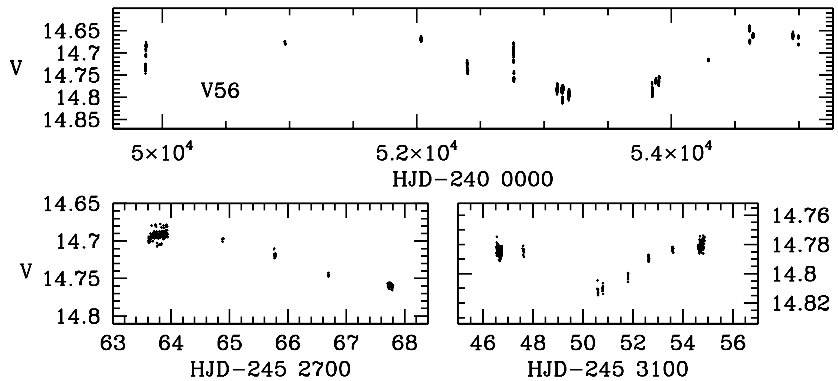

Fig. 10. Light curves of the variable V56.

sociated with one from the close pair of X-ray sources detected by Bassa *et al.* (2004). The optical variability of this object may indicate its binary nature. If V56 is indeed a binary, then the rapid rotation of the giant component may result in substantial chromospheric activity and associated X-ray emission. The star was identified as a radial velocity variable by Sommariva *et al.* (2009, object No. 34848 in their Table 4). Two radial-velocity measurements performed 80 days apart yielded 66.75 ± 0.12 km/s and 64.31 ± 0.07 km/s. These values both confirm the variability of V56 and prove that it is a radial-velocity member of M4.

The hot subdwarfs V46 and V63 are proper motion members of M4. Both the stars have blue $U-B$ colors (Mochejska *et al.* 2002). The binary nature of V46 was discussed in some detail by O'Toole *et al.* (2006). Our data show that the light curve of this variable was very stable over the time interval of 14 years (Fig. 7). The *V*-band luminosity of the second subdwarf was systematically increasing from 17.71 mag in 1995 to 17.68 mag in 2009, however we did not detect any periodicity in its light curve.

5. Blue and Yellow Stragglers

Our accurate photometry supplemented with proper motion memberships of Zloczewski *et al.* (2012) allows to select a very clean sample of blue and yellow stragglers (BSs and YSs) belonging to the cluster. Fig. 11 shows the relevant region of the CMD, only proper motion members of M4 are shown. For reference we also plot a 2.5 Gyr isochrone with $[\mathrm{Fe/H}] = -1.2$ from the Dartmouth data base (Dotter *et al.* 2008). To match the lower main sequence the isochrone was shifted assuming a reddening $E(B-V) = 0.392$ mag and distance modulus $DM = 12.81$ mag. This isochrone is a good fit to the lower main sequence of M4 on our CMD. The sequence of BSs emerges from the main sequence below the cluster turnoff at $V \approx 17.3$ mag and extends to $V = 14.6$ mag. It includes 38 BSs with $B-V < 0.81$ mag and eight YSs located above the subgiant branch. As it can be seen in Fig. 11, masses of these objects range from 0.8 $M_\odot$ to to 1.4 $M_\odot$, where

0.8 $M_{\odot}$ is the turnoff mass of M4 (Kaluzny *et al.* 2013 and references therein). This estimate is based on the assumption that BSs and YSs follow the standard relation between mass, color and luminosity.

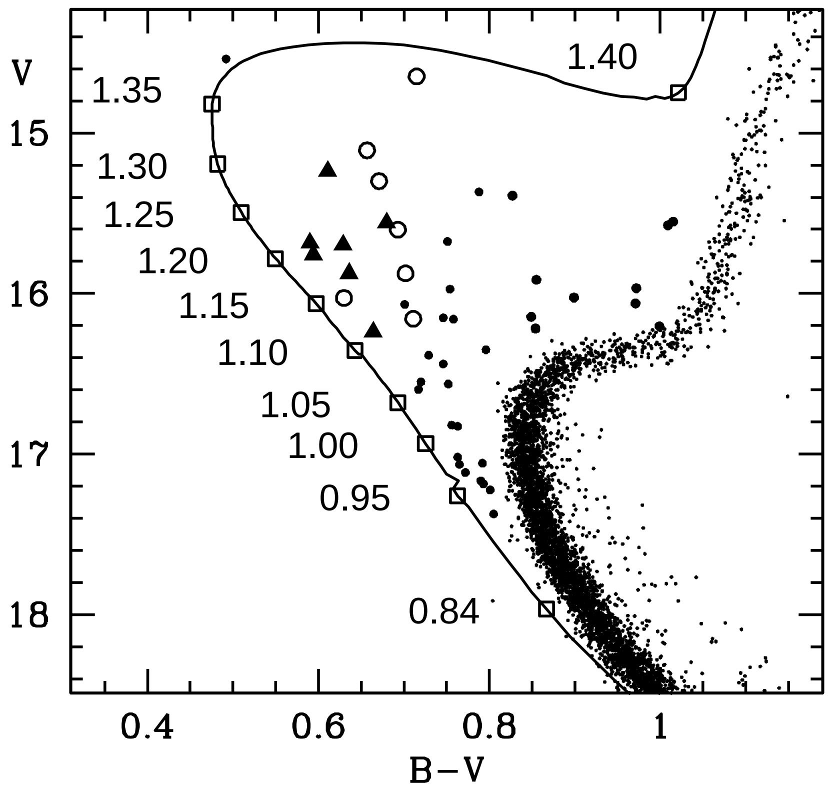

Fig. 11. Color–magnitude diagram for proper motion members of M4. Positions of blue and yellow straglers are marked with triangles (fast rotators), circles (slow rotators) and large dots (objects with unknown rotation rates). A 2.5 Gyr isochrone is also shown, with stellar masses marked at selected locations.

The stragglers are thought to originate either as products of the evolution of close binary systems or *via* stellar collisions and direct merging (McCrea 1964, Hills and Day 1976). The first scenario may lead to a coalescence of the components, but an end product in the form of a detached binary emerging from the mass exchange phase is also possible.

Coalescence should result in fast rotation of the merger product. Lovisi *et al.* (2010) obtained $V\sin i$ values for 20 BSs from M4. They found $V_{\rm rot}\sin i > 50$ km/s for eight "fast rotators" and lower values of $V_{\rm rot}\sin i$ for the remaining 12 objects. Our sample of stragglers includes 16 stars from Lovisi's survey. Seven of these are fast rotators and proper motion members of the cluster. Lovisi's BSs 2000121, 43765 and 2000085 correspond to V53, V61, and V68, respectively. For the remaining objects with $V_{\rm rot}\sin i > 50$ km/s we found no evidence for photometric variability. Lovisi's BS 2000106 turned out to be a field star. The remaining eight "slow rotators" from Lovisi's list are proper motion members of M4. Fig. 11 suggests that the fast rotators are relatively unevolved in the sense of stellar evolution (they belong to the bluest BSs). This in turn may suggest that they are products of a recent (in case of V53 even ongoing) mass exchange in binary systems. This conjecture can be verified by time-series spectroscopic observations of our BS/YS sample.

Eclipsing BSs have been found in several clusters, however the membership status remains to be established for many of them. Those with confirmed cluster membership include Algols NJL5 = V192 in Omega Cen (Niss *et al.* 1978, Bellini *et al.* 2009), V228 in 47 Tuc (Kaluzny *et al.* 2007), and V60 in M55 (Rozyczka *et al.* 2013), as well as a number of contact systems. We have examined the population of contact binaries in seven clusters with proper motion data to find that just 15 of them are blue stragglers, of which 10 belong to the very massive and atypical cluster Omega Cen (Kaluzny and Rozyczka, in preparation). We conclude that in nearby well studied clusters not more than a few percent of BSs are eclipsing binaries. M4 seems to follow this trend: among the 45 BS/YS in M4 there is just one eclipsing binary, the contact system V53.

The accuracy of our photometry is sufficient to detect periodic variability at a milli-magnitude level for stars with $V < 17$ mag and periods up to a few days, as expected in close binaries with an ellipsoidal effect. We failed to find any such variability. However, this does not exclude the possibility that the potential binary stragglers are well detached. To verify such a hypothesis, a radial velocity survey of M4 is needed, similar to the spectroscopic study of the old open cluster NGC 188 which led to the detection of 15 binary blue stragglers with orbital periods ranging from a few days to 10^4 days (Geller and Mathieu 2012). Eight binary BSs in NGC 188 are SB1 systems whose secondary components have masses estimated at 0.6 $M_\odot$ (Geller and Mathieu 2012). It is natural to assume that such objects are white dwarfs. If this is true, then the essential factor responsible for the formation of those blue stragglers must have been mass exchange. One may wonder if binaries hosting white dwarfs are present also among BS/YS in M4.

6. Summary

We monitored M4 photometrically from 1995 untill 2009, obtaining over 3000 CCD images of the cluster. Our *V*-band photometry is accurate to within 5 mmag at the turnoff ($V = 17$ mag), and to within 50 mmag at $V = 20$ mag. The collected data are accurate enough to measure the differential reddening $\delta E(B-V)$ across the surveyed field, which varies between -0.053 mag and $+0.011$ mag (with negative values corresponding to higher reddening). $\delta E(B-V)$ is specified with respect to a reference subfield, for which we have found $E(B-V) = 0.392$ mag using the low-extinction globular cluster NGC 6362 as an intermediary. Accounting for $\delta E(B-V)$ and using the membership catalog of Zloczewski *et al.* (2012), we have derived a very clean color–magnitude diagram of M4 with sharply defined principal features and a clearly visible binary main sequence. We also selected a clean sample of a few dozen of blue and yellow stragglers. Being proper-motion members of M4, they can be used for a spectroscopic study which might shed light on the origins of these populations of stars.

We have obtained light curves of 22 variable stars, ten of which are newly detected. Accurate periods are found for all but two variables. Nineteen variables are firm or likely proper-motion members of the cluster. Among these there are four detached binaries, seven contact binaries, two subdwarfs, one binary which may be either semidetached or contact, and two SX-Phe pulsators. The remaining three cluster variables (V52, V56, and V58) are most likely binaries. The binary nature of V56 is suggested by seasonal variations of the average luminosity and a low amplitude variability on a time scale of ≈ 10 days. Such a behavior can be expected from a red-giant primary, whose rapid synchronous rotation results in a high chromospheric activity. In the case of V52 a periodic modulation of the luminosity with $P \approx 0.78$ d is observed, which may be attributed to the ellipsoidal effect. The light curve of V58 was obtained by Kaluzny *et al.* (2012), who identified this star with the X-ray source CX1 from the list of Bassa *et al.* (2004). They argue that this system is composed of a neutron star and a low-mass companion which has lost most of its hydrogen envelope.

Besides V58, another four cluster variables are either firm or likely optical counterparts of X-ray sources: V56 seems to be associated with CX5 or CX9 from the same list, and the optical counterparts of CX13, CX15, and CX30 are, respectively, eclipsing binaries V48, V49, and V65. V52 is not associated with any known X-ray source, however on May 3rd, 2006 it flared for about 90 min with an amplitude $\Delta V = 0.11$ mag. This type of activity also should be accompanied by an X-ray emission. Among the three field objects which complete the sample of detected variables there are are two SX-Phe pulsators and a contact binary.

We find that all but one of the contact (EW) systems show season-to-season variations of the average luminosity with an amplitude of more than 0.1 mag. Such behavior can be explained by magnetic cycles five to ten years long. Interestingly, their periods are similar to that of the solar cycle despite a huge difference in rotation rates. Another interesting finding is that the contact binaries appear exclusively among evolved stars which suggests that at least in globular clusters the principal factor enabling EW systems to form from close but detached binaries is stellar evolution. The estimated frequency of occurrence of EW systems in M4, $0.12 \pm 0.05\%$, is consistent with the value of 0.2% observed in the solar neighborhood. Two contact binaries with total eclipses, V48 and V53, have very low mass ratios of $q = 0.148$ and $q = 0.060$, respectively. The latter value poses a challenge for the current theory, according to which $q = 0.09-0.08$ is the lower limit for tidally stable contact binaries.

The detached binaries V65 and V66, located at the turnoff, were additionally subject to a thorough spectroscopic survey. Their detailed analysis including the determination of absolute parameters and ages can be found in Kaluzny *et al.* (2013). The light curves of all variables as well as other data presented in this paper are available online at *http://case.camk.edu.pl/results/index.html*.

Acknowledgements. We thank Loredana Lovisi for sending us the coordinates of M4 stragglers with measured rotation rates. JK and MR were partly supported by the National Science Center grant 2012/05/B/ST9/03931. IBT was supported by NSF grant AST-0507325.

REFERENCES

Alard, C. 2000, *A&AS*, **144**, 363.
Alard, C., and Lupton, R. 1998, *ApJ*, **503**, 325.
Anderson, J., *et al.* 2008, *AJ*, **135**, 2055.
Arbutina, B. 2012, *Publ. Astron. Obs. of Belgrade*, **91**, 391.
Bassa, C., *et al.* 2004, *ApJ*, **609**, 755.
Bellini, A., Piotto, G., Bedin, L.R., Anderson, J., Platais, I., Momany, Y., Moretti, A., Milone, A.P., and Ortolani, S. 2009, *A&A*, **493**, 959.
Carretta, E., Bragaglia, A., Gratton, R., D'Orazi, V., and Lucatello, S. 2009, *A&A*, **508**, 695.
Clement, C., *et al.* 2001, *AJ*, **122**, 2587.
Cudworth, K.M., and Rees, R. 1990, *AJ*, **99**, 1491.
Dotter, A., Chaboyer, B., Jevremović, O., Kostov, V., Baron, E., and Ferguson, J.W. 2008, *ApJS*, **178**, 89.
Dotter, A., *et al.* 2010, *ApJ*, **708**, 698.
Geller, A.M., and Mathieu, R.D. 2012, *AJ*, **144**, 54.
Hills, J.G, and Day, C.A. 1976, *Astrophysical Letters*, **17**, 87.
Harris, W.E. 1996, *AJ*, **112**, 1487.
Hendricks, B,. Stetson, P.B., VandenBerg, D.A., and Dall'Ora, M. 2012, *AJ*, **144**, 25.
Kaluzny, J., and Krzeminski, W. 1993, *MNRAS*, **264**, 785.
Kaluzny, J., Thompson, I.B., and Krzeminski, W. 1997, *AJ*, **113**, 2219.
Kaluzny, J., Thompson, I.B., Rucinski, S.M., Pych, W., Stachowski, G., Krzeminski, W., and Burley, G.S. 2007, *AJ*, **134**, 541.
Kaluzny, J., and Thompson, I.B. 2009, *Acta Astron.*, **59**, 273.
Kaluzny, J., Thompson, I.B., Krzeminski, W., and Zloczewski, K. 2010, *Acta Astron.*, **60**, 245.
Kaluzny, J., Rozanska, A., Rozyczka, M., Krzeminski, W., and Thompson, I.B. 2012, *ApJ*, **750**, L3.
Kaluzny, J., *et al.* 2013, *AJ*, **145**, 43.
Kubiak, M., Udalski, A., Szymanski, M. 2006, *Acta Astron.*, **56**, 253.
Landolt, A. 1992, *AJ*, **104**, 372.
Lovisi, L., *et al.* 2010, *ApJ*, **719**, L121.
McCrea, W.H. 1964, *MNRAS*, **128**, 147.
Mochejska, B.J., Kaluzny, J., Thompson, I., and Pych, W. 2002, *AJ*, **124**, 1486.
Mochnacki, S.W., and Doughty, N.A. 1972, *MNRAS*, **156**, 51.
Monelli, M. *et al.* 2013, *MNRAS*, **431**, 2126.
Nef, P.D., and Rucinski, S.M. 2008, *MNRAS*, **385**, 2239.
Niss, B., Jorgensen, H.E., Laustsen, S. 1978, *A&AS*, **32**, 387.
O'Toole, S.J., Napiwotzki, R., Heber, U., Drechsel, H., Frandsen, S., Grundahl, F., and Bruntt, H. 2006, *Baltic Astronomy*, **15**, 610.

Prŝa, A., and Zwitter, T. 2005, *ApJ*, **628**, 426.
Rasio, F.A. 1995, *ApJ*, **444**, L41.
Reed, B.C., Hesser, J.E., and Shawl, S.J. 1988, *PASP*, **100**, 545.
Rozyczka, M., Kaluzny, J., Thompson, I.B, Rucinski, S.M., Pych, W., and Krzeminski, W. 2013, *Acta Astron.*, **63**, 67.
Rucinski, S.M., Lu, W., Mochnacki, S.W., Ogloza, W., and Stachowski, G. 2001, *AJ*, **122**, 1974.
Rucinski, S.M., and Paczynski, B. 2002, *IBVS*, 5321.
Rucinski, S.M. 2002, *PASP*, **114**, 1124.
Schlegel, D.J., Finkbeiner, D.P., and Davis, M. 1998, *ApJ*, **500**, 525.
Schlafly, E.F., *et al.* 2010, *ApJ*, **725**, 1175.
Stetson, P.B. 1987, *PASP*, **99**, 191.
Stetson, P.B. 1990, *PASP*, **102**, 932.
Stetson, P.B. 2000, *PASP*, **112**, 925.
Schwarzenberg-Czerny, A. 1996, *ApJ*, **460**, L107.
Schwarzenberg-Czerny, A., and Beaulieu, J-Ph. 2006, *MNRAS*, **365**, 105.
Sommariva, V., Piotto, G., Rejkuba, M., Bedin, L.R., Heggie, D., Mathieu, R.D., and Villanova, S. 2009, *A&A*, **493**, 947.
Stępień, K., and Gazeas, K. 2012, *Acta Astron.*, **62**, 153.
Zacharias, N., *et al.* 2010, *AJ*, **139**, 2184.
Zinn, R. 1985, *ApJ*, **293**, 424.
Zinn, R., and West, M.J. 1984, *ApJS*, **55**, 45.
Zloczewski, K., Kaluzny, J., Rozyczka, M., Krzeminski, W., and Mazur, B. 2012, *Acta Astron.*, **62**, 357.